Ultrasound in Med. & Biol., Vol. 30, No. 6, pp. 735–743, 2004

0301-5629/04/$–see front matter

ELSEVIER

doi:10.1016/j.ultrasmedbio.2004.03.016

● *Original Contribution*

VASCULAR FLOW AND PERFUSION IMAGING WITH ULTRASOUND CONTRAST AGENTS

MATTHEW BRUCE,*‡ MIKE AVERKIOU,‡ KLAUS TIEMANN,† STEFAN LOHMAIER,†
JEFF POWERS‡ and KIRK BEACH*
*Department of Bioengineering, University of Washington, Seattle, WA, USA; †Department of Cardiology, University of Bonn, Bonn, Germany; and ‡Philips Ultrasound, Bothell, WA, USA

(*Received* 4 *December* 2003; *revised* 30 *March* 2004; *in final form* 30 *March* 2004)

Abstract—Current techniques for imaging ultrasound (US) contrast agents (UCA) make no distinction between low-velocity microbubbles in the microcirculation and higher-velocity microbubbles in the larger vasculature. A combination of radiofrequency (RF) and Doppler filtering on a low mechanical index (MI) pulse inversion acquisition is presented that differentiates low-velocity microbubbles (on the order of mm/s) associated with perfusion, from the higher-velocity microbubbles (on the order of cm/s) in larger vessels. *In vitro* experiments demonstrate the ability to separate vascular flow using both harmonic and fundamental Doppler signals. Fundamental and harmonic Doppler signals from microbubbles using a low-MI pulse-inversion acquisition are compared with conventional color Doppler signals *in vivo*. Due to the lower transmit amplitude and enhanced backscatter from microbubbles, the *in vivo* signal to clutter ratios for both the fundamental (−11 dB) and harmonic (−4 dB) vascular flow signals were greater than with conventional power Doppler (−51 dB) without contrast agent. The processing investigated here, in parallel with conventional pulse-inversion processing, enables the simultaneous display of both perfusion and vascular flow. *In vivo* results demonstrating the feasibility and potential utility of the real-time display of both perfusion and vascular flow using US contrast agents are presented and discussed. (E-mail: mbruce@u.washington.edu)

Key Words: **Ultrasound contrast agents, Doppler, Color Doppler, Blood flow.**

INTRODUCTION

The major motivation for continued research of ultrasound (US) contrast agents (UCA) over the past 20 years has been the possibility of detecting perfusion with US. The detection of tissue perfusion would yield information about organ viability and function enabling new applications for US. As a result, methods dedicated explicitly to the detection of blood flow in larger vessels (diameters > 2 mm) with contrast agents have received little attention.

Despite increases in sensitivity of color flow systems, clinical situations exist in which the detection of blood flow in the vasculature is still problematic (Powers et al. 1996). Color-flow systems used for the detection of vascular flow are challenged by the weak backscatter of blood relative to tissue (-40 to -60 dB). The practical consequence of this challenge is limited sensitivity to low-velocity flow in smaller vessels (diameter < 2 mm), blood flow in deep vessels ($>$ 10 cm) and flow in regions with tissue motion. One approach to overcome these limitations is to inject brighter ultrasonic scatterers into the vascular system. Gas-filled microbubbles are a reflector in clinical use. Unfortunately, conventional color Doppler has proven to be a poor method of detecting flowing microbubbles (Powers et al. 1996). Blooming over vessels walls and uncorrelated Doppler signals due to microbubble destruction are examples of the difficulties encountered (Powers et al. 1996).

Researchers have manipulated methods developed to detect perfusion with microbubbles to better image vascular flow. Two general approaches have been applied to visualize blood flow in larger vessels with current contrast agent imaging methods. Low mechanical index (MI) (< 0.12) harmonic techniques have been devised to visualize nearly stationary micro-

Address correspondence to: Matthew Bruce, M.D., Philips Medical Systems, 22100 Bothell Everett Highway, P.O. Box 3003, Bothell, WA 98041 USA. E-mail: mbruce@u.washington.edu

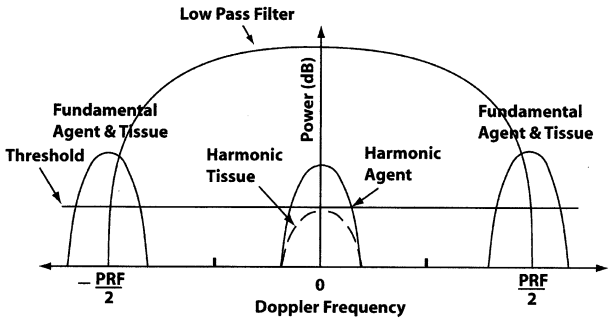

Fig. 1. Doppler spectrum of a pulse-inversion acquisition with illustration of conventional pulse-inversion processing, composed of a low-pass filter to remove the fundamental and a threshold to remove harmonic tissue. The fundamental signal has been reduced by RF filtering at the second harmonic.

bubbles in the microcirculation in real-time with frame rates exceeding 8 Hz. Following a bolus injection, the larger feeding vessels of the vascular tree can be visualized until the microcirculation fills. After the microcirculation is filled, microbubbles in the parenchyma obscure visualization of larger arterial and venous vessels. This method provides momentary visualization of the larger arterial vessels at the beginning of the bolus (~5–30 s). Another approach has been to simply raise the transmitted amplitude so that the low-velocity microbubbles are destroyed, leaving only microbubbles with high enough velocities in larger vessels to replenish sample volumes. This method destroys the agent in the microcirculation, relies on a delicate balance between signal and destruction and is unable to display perfusion information.

Real-time visualization of vascular blood flow with contrast at a low MI would enable simultaneous detection of perfusion and simplify detection of vascular flow over current methods. The display of larger vessels throughout a bolus or infusion would provide landmarks during a contrast scan. Improved vascular visualization over color Doppler would have a clinical impact on a number of applications, such as liver lesion detection and characterization, cancer therapy monitoring and stroke management (Pohl et al. 2000; Wilson and Burns 2001). The goal of this work is to add vascular flow information to existing perfusion images created with UCA. Using a pulse-inversion acquisition, a method is presented that extracts in real-time both vascular flow and perfusion information.

This paper is organized as follows. First, conventional pulse inversion for imaging perfusion is presented. An algorithm for detecting harmonic and fundamental flow components from a pulse-inversion acquisition using microbubbles is presented. *In vitro* experiments demonstrate the ability of the method to separate stationary tissue and microbubbles from flowing microbubbles with both the fundamental and harmonic Doppler signals. *In vivo* experimental data from a human liver are used to quantify and evaluate the harmonic and fundamental flow components expected in clinical practice. A comparison of clutter and flow amplitudes is made against conventional power Doppler without contrast.

METHODS

Pulse inversion for perfusion

A pulse-inversion acquisition consists of transmitting *n* pulses down each direction line, with each subsequent pulse inverted. The resulting effect on the Doppler spectrum is that odd harmonic components are modulated to Nyquist and even harmonic components are moved to zero (Hope Simpson et al. 1999). The phase shift experienced by the inverted pulses at the second harmonic is twice that at the fundamental, because the received second harmonic signal is twice the RF frequency of the fundamental. An 180° phase shift, the inversion, at the fundamental corresponds to a 360° phase shift at the second harmonic, which aliases back to zero frequency in the Doppler spectrum (Bruce et al. 2000).

The detection of nearly stationary microbubbles in the microcirculation is accomplished by applying a low-pass filter to remove the fundamental component (Fig. 1). The remaining harmonic tissue can be removed by a simple threshold of the resulting power. The fundamental component illustrated in Fig. 1 has been diminished by RF filtering around the second harmonic (see Fig. 2). This RF filtering helps remove fundamental tissue motion that can leak into the pass band of the low-pass filter. The utility of pulse inversion arises from the ability to separate harmonic sig-

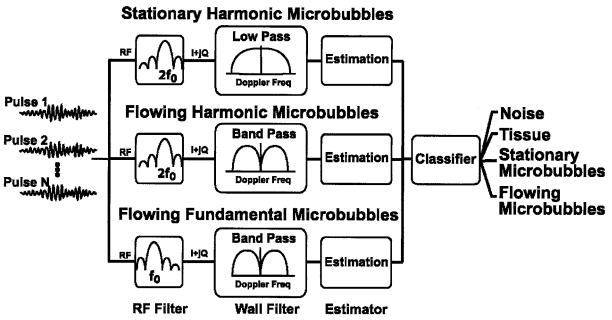

Fig. 2. Illustration of parallel processing for the simultaneous detection and display of perfusion and vascular flow with UCA. The top path illustrates conventional pulse-inversion processing.

nals overlapping the fundamental in the RF spectrum. This separability enables harmonic imaging using broadband transmit waveforms for greater axial resolution. Otherwise, a narrowband transmit is required for harmonic imaging to prevent the overlap of second harmonic and fundamental components (Averkiou 2000).

The discovery that microbubbles could be differentiated from tissue using a low-output power led to the real-time estimation of perfusion (Averkiou et al. 2001). Prior to this discovery, normal diagnostic US output powers were used (MI $>$ 1.0), which destroyed the microbubbles.

The associated requirement for nondestructive detection of microbubbles in the microcirculation, enabling real-time visualization of perfusion, limits the MI to below 0.10 (Tiemann et al. 2001). Full-sector fields-of-view are generally used in UCA perfusion imaging. To maintain clinically usable frame rates with large acquisition sectors, Doppler shifts from higher-velocity microbubbles must be detected using short ensemble lengths (2–6). These design constraints raise the question of whether vascular flow can be detected with contrast with equal or greater sensitivity and penetration relative to conventional color-flow imaging without contrast.

Pulse inversion for flow

This section describes processing to discriminate higher-velocity microbubbles ($>$ 0.5 cm/s) in the macrovasculature from those in the microcirculation using a pulse-inversion acquisition. The 2-D Fourier transform of a Doppler acquisition indexed in fast and slow time shows the position of each Doppler spectral component in the RF spectrum (Evans and McDicken 2000). The 2-D discrete Fourier transform of an array indexed in sample depth and pulse number of a Doppler acquisition is defined as:

$$P(k_{rf},k_{\mathrm{Dop}}) = \frac{1}{N_{El}N_{\mathrm{depth}}} \times \sum_{n_{\mathrm{Dop}}=0}^{N_{\mathrm{EL}^{-1}}} \sum_{n_{\mathrm{depth}}=0}^{N_{\mathrm{depth}^{-1}}} x(n_{rf},n_{\mathrm{Dop}}) e^{-j\frac{2\pi}{N_{\mathrm{depth}}}k_{rf}n_{\mathrm{depth}}} e^{-j\frac{2\pi}{N_{EL}}k_{\mathrm{Dop}}n_{\mathrm{Dop}}} \quad (1)$$

where $x(n_{rf},n_{\mathrm{Dop}})$ is the array of RF samples for each Doppler acquisition (n_{Dop}), N_{EL} is the ensemble length, N_{depth} is the number of depth samples and k_{Dop} and k_{RF} are the spectral indices of the Doppler and RF spectra. Figure 3 is a graphic illustration of a pulse-inversion 2-D power spectrum from a sample volume containing both stationary tissue with microbubbles and flowing microbubbles. The transmit frequency in Fig. 3 is 1.7 MHz.

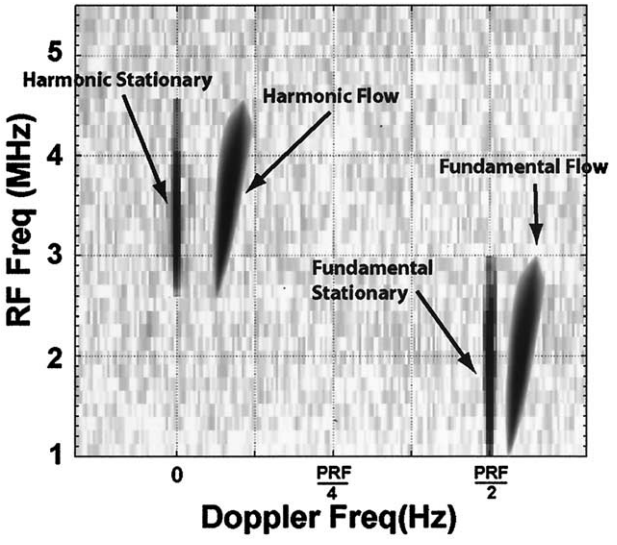

Fig. 3. 2-D Doppler RF spectrum of a pulse-inversion acquisition over a sample volume containing both stationary tissue or microbubbles and flowing microbubbles.

Stationary targets generate a zero Doppler frequency. The second harmonic component is centered at zero frequency along the Doppler axis and at twice the transmit frequency (3.4 MHz) along the RF axis. The fundamental component is centered at Nyquist along the Doppler axis due to the pulse inversion process, and centered at the transmit frequency (1.7 MHz) along the RF axis. If there are scatterers moving in the sample volume, each frequency component of the scattered pulse exhibits a Doppler shift given by the Doppler equation ($f_d = 2\ \nu/cf_{RF}$). The vertical spectral lines tilt along lines with slopes of $2\ \nu/c$ (Wilson 1991). The broadening of the spectral line arises due to moving targets passing through the finite sample volume. The increase in spectral broadening with RF frequency reflects the fact that the effective sample volume shrinks with increasing RF frequency (Wilson 1991).

The isolation of second harmonic signals with Doppler shifts can be achieved as follows. To detect second harmonic signals with Doppler shifts, a bandpass RF filter centered at the second harmonic frequency attenuates the fundamental component. A bandpass filter in the Doppler domain removes the remaining stationary second harmonic and fundamental components at DC and Nyquist, respectively. Similar processing can be used to separate the fundamental vascular flow component.

Wall filter for pulse-inversion flow

The wall filter operation can be cast as a matrix multiplication of the discrete Doppler time series:

$$y = Ax \tag{2}$$

where A is a $N \times N$ matrix with N equaling the ensemble length and x is a $N \times 1$ vector with elements of values from each pulse at a particular depth. The bandpass response of the Doppler filter illustrated in Fig. 2 can be achieved by cascading two high-pass wall filters in series:

$$A = A_{\text{Fund}} \begin{bmatrix} -1 & 0 & \cdots & \\ 0 & 1 & 0 & \\ \vdots & 0 & -1 & \ddots \\ & & \ddots & \ddots \end{bmatrix} A_{\text{Harm}} \tag{3}$$

where A_{Harm} and A_{Fund} are NxN matrices with high-pass frequency characteristics. The middle diagonal matrix acts as a mixing matrix to translate the fundamental at Nyquist down to DC. The utility of eqn (3) is that existing wall filter design techniques can be used togenerate A_{Harm} and A_{Fund} (Bjaerum et al. 2002). In addition, A_{Harm} and A_{Fund} may have different frequency responses. Zero order least square regression filters were used for both A_{Harm} and A_{Fund} in the following experiments. The dynamic range of fundamental clutter is much higher than that of the second harmonic (see the Results section). The resulting rank of A must be greater than or equal to two to estimate frequency or one to estimate power. This limits the dimension of the null space of A or subspace allocated to the removal of clutter (cut-off frequency) considering that ensemble lengths of three to six are used. Also, because A_{Harm} acts first on x, it must have a nearly linear phase response for A_{Fund}. Otherwise, low-frequency stationary clutter signals are modulated into the pass band of A_{Fund}.

Fundamental and harmonic flow components

The discrimination of microbubbles from tissue has relied solely on their differences of nonlinearity. For the detection of flowing microbubbles, the fundamental signal can be used because a wall filter can remove stationary tissue. Due to the larger signal amplitude and lower attenuation relative to the harmonic, the fundamental signal is expected to have more penetration and sensitivity. Figure 2 illustrates parallel signal paths with which perfusion and vascular flow signals can be detected and displayed simultaneously from a pulse-inversion acquisition. The top signal path illustrates conventional pulse inversion processing for perfusion. The other two signal paths detect harmonic and fundamental signals for higher-velocity microbubbles in larger vasculature. Parameters from each of these signal paths are then used for the discrimination of tissue, perfusion, noise and vascular flow. The fundamental and harmonic flow components each have advantages and disadvantages important to imaging flow, to be discussed in the Results section.

MATERIALS

In vitro *experiment*

An HDI 5000 US system (Philips Ultrasound, Bothell, WA) equipped with a C5-2 curvilinear transducer was used for all the experiments. For proof of principle, a flow phantom was imaged with flowing microbubbles and stationary microbubbles to simulate perfusion. A Masterflex 77201 pump (Cole Parmer Co. Barrington, IL) was used to pump diluted contrast agent through a flow phantom with an 8-mm tube (model 523A, ATS Labs Inc., Bridgeport, CT). The

flow circuit contained 0.05 mL of the contrast agent Optison® (Amersham Health AS, Oslo, Norway) diluted in 1 l of 0.9% saline. A single line pulse-inverted transmit sequence was acquired, enabling the collection of enough pulses to estimate the Doppler spectrum. A pulse-inverted sequence was transmitted down a single line using a 1.7-MHz three-cycle pulse at a pulse-repetition frequency (PRF) of 4000 Hz. The center of the tube intersected the acquired scan line at a depth of 7 cm and at an angle of 60° relative to the transmit beam. For acquisitions with flow, the mean and peak Doppler angle-corrected velocities were measured to be 5.0 and 10.0 cm/s, respectively, using spectral Doppler on the HDI 5000 US system. The output power was set at an MI of 0.12. Beam-formed RF data from 340 pulses were acquired for two flow states. One set of RF data was acquired with the flow pump turned off and with the flow tube filled with contrast to simulate perfusion. Another set of RF data was acquired with flow pump turned on. For this acquisition with flow, the angle-corrected peak velocity was measured to be 11.0 cm/s, using spectral Doppler on the HDI 5000. Before each data acquisition, transmit was temporarily suspended to avoid microbubble destruction.

In vivo *experiment*

To test clinical feasibility, the liver of a healthy volunteer was imaged during a bolus injection of contrast agent. An HDI 5000 US system was again used equipped with the C5-2 transducer. A typical dose in clinical use of the contrast agent Definity® (Bristol-Myers Squibb, New York, NY) was injected (0.2 mL followed by a 5-mL saline flush at 2 mL/s). A four-pulse pulse-inverted sequence was transmitted using a 1.7-MHz three-cycle pulse at a PRF of 1 kHz and an MI of 0.07. Beam-formed RF data was then acquired near the peak of the portal phase of the injection (when contrast agent enters the liver *via* the portal vein).

After contrast agent had cleared the liver, RF data were collected using the conventional power Doppler mode without contrast for comparison of vascular flow sensitivity. The US system was set up in a low-velocity power Doppler mode optimization. This optimization consisted of a 2.5-MHz pulse with a PRF of 1 kHz, and an ensemble length of 10. The acquisitions with and without contrast were ECG-triggered to enable comparison of flow with contrast against conventional power Doppler flow without contrast at the same point in the cardiac cycle. This experiment was done with approval of the University of Washington's human subjects division.

RESULTS

The *in vitro* experiment was performed using a single scan line acquisition to enable visualization of both the Doppler and RF spectral content. The algorithms for fundamental and harmonic flow could then be tested using data with known RF and Doppler spectral structures. The signal paths of Fig. 2 for perfusion, harmonic flow and fundamental flow were tested by processing the 340 pulses in groups of effective ensemble lengths of four to produce an M-mode image for each flow state.

A meaningful assessment of clinical utility of the algorithms for harmonic and fundamental flow can only happen with *in vivo* microbubble concentrations and transmit amplitudes used for perfusion. The *in vivo* experiment provides harmonic and fundamental signal-to-noise (SNR) and signal-to-clutter ratios experienced in a clinical scenario to detect perfusion with contrast. The harmonic and fundamental flow signals with contrast are compared against blood flow signals detected with conventional power Doppler without contrast.

In vitro *results*

The 2-D power spectra in Fig. 4 were estimated using a 2-D array of 340 Doppler pulses by 7-mm section of RF. Figure 4a shows the 2-D and 1-D Doppler and RF spectra of a section of RF from a region-of-interest (ROI) located in the tissue-mimicking material just above the tube (5.5 cm). Figure 4b shows spectra of stationary microbubbles in the tube with no flow. The same spectral structure is observed as for tissue, with the exception of 20-dB increased second harmonic signal. The fundamental signals, centered at Nyquist in the Doppler spectrum, of tissue and stationary microbubbles are at the same level. This result illustrates why harmonic imaging techniques have been used for the discrimination between tissue and microbubbles. Figure 4c shows the spectra of flowing microbubbles in the tube, with similar 2-D spectral content of Fig. 3. The peaks of the fundamental and harmonic spectral Doppler components have shifted off from Nyquist by 150 Hz and off from DC by 250 Hz. The fundamental and harmonic Doppler shifts correspond to Doppler angle-corrected velocities of 10 and 11 cm/s, respectively, matching the measured velocity by spectral Doppler of the US system. Figure 4 illustrates the spectral content described in the Methods section and provides rationalization for the processing described for the separation of vascular flow (bottom signal paths of Fig. 3).

In addition to the fundamental and second harmonic signals, there is a small uncorrelated signal spread across the Doppler spectrum centered around the fundamental

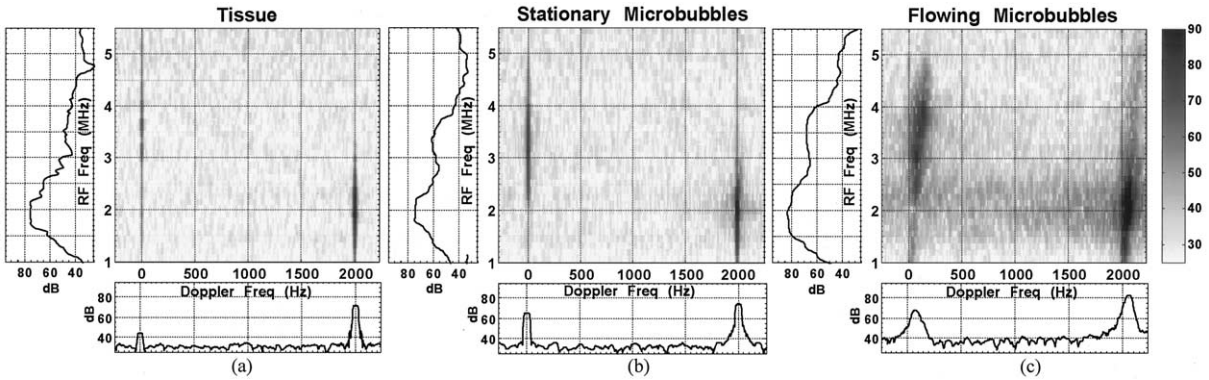

Fig. 4. RF and Doppler 1-D spectra (vertical and horizontal plots, respectively) and 2-D RF Doppler spectra from pulse-inversion acquisitions of (a) tissue, (b) stationary microbubbles in tube, and (c) flowing microbubbles in tube.

RF frequency, roughly 5 dB above the noise floor. This uncorrelated signal is likely due to microbubble disruption in the sample volume, observed even at this low MI (Chomas et al. 2001).

Figure 5 shows M-mode images made by breaking the acquisition of 340 pulses into 85 ensembles of length four for both stationary (Fig. 5a–c) and flowing microbubbles (Fig. 5d–f). All the images are displayed with a dynamic range of 42 dB. The tube resides between depths of 65 mm and 73 mm. Figure 5a and d show conventional pulse-inversion processing (top signal path of Fig. 2) for stationary and flowing microbubbles. Tissue harmonic signals appear above and below the tube. Figure 5b and e shows the fundamental Doppler signal from the bottom processing path of Fig. 2 of stationary and flowing microbubbles, respectively. Figure 5c and f shows the removal of the harmonic stationary tissue and microbubble signals seen in Fig. 5a and d. The SNRs for the harmonic and fundamental are 22 and 40 dB, respectively. Figure 5 illustrates higher velocity microbubbles can be differentiated from stationary microbubbles using tissue and a low-MI pulse-inversion acquisition.

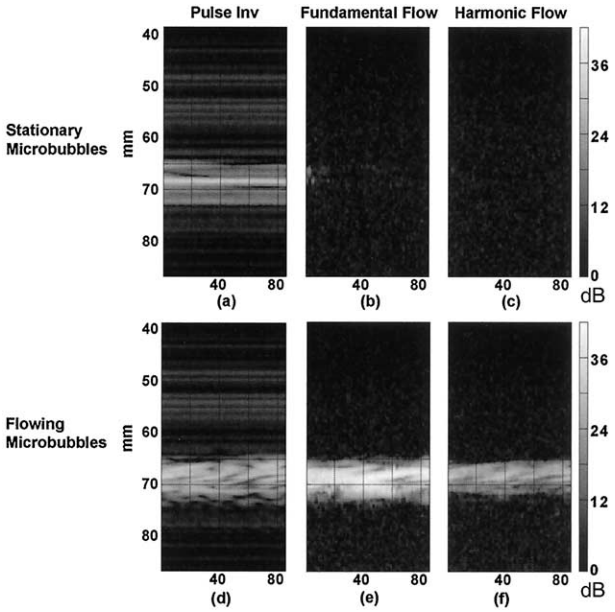

Fig. 5. M-mode images (depth vs. time) of stationary microbubbles (a)–(c) and flowing microbubbles (d)–(e). The grey scale shows the results of (a) and (d) pulse inversion imaging, (b) and (e) harmonic flow, and (c) and (f) fundamental flow. All images were processed with an ensemble length of four pulses. The x-axis is in ms.

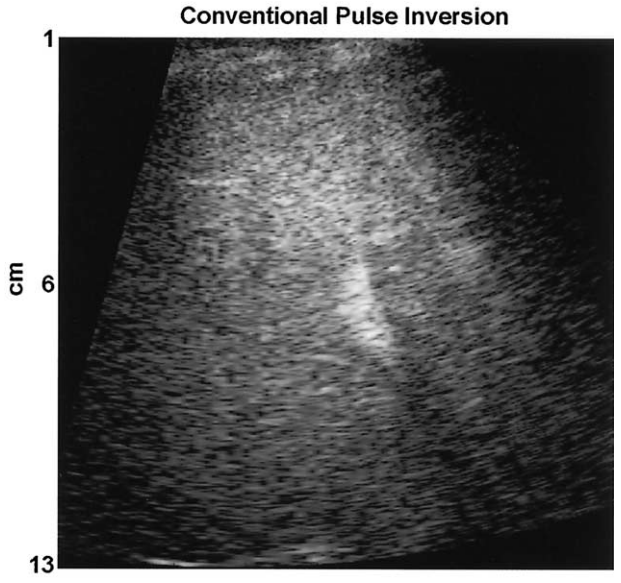

Fig. 6. Perfusion image of the liver with contrast processed using conventional pulse-inversion processing (top signal path of Fig. 2) with a displayed dynamic range of 30 dB.

In vivo *results*

This section investigates the clinical practicality of detecting perfusion and vascular flow in real-time with microbubbles. Low-MI harmonic and fundamental vascular flow signals with contrast are compared against conventional power Doppler in the liver. Figure 6 shows the perfusion image obtained through conventional pulse-inversion processing using UCA. The portal vein is visible in the center of the image, but the rest of the larger vasculature is obscured due to microbubbles residing in the microcirculation. The diaphragm can be seen at the bottom of Fig. 6 at 13 cm. Figure 7a shows liver images of conventional power Doppler without contrast. Figure 7b shows fundamental vascular flow with contrast analogous to Fig. 5e for the *in vitro* experiment. Figure 7c shows harmonic vascular flow with contrast analogous to Fig. 5f for the *in vitro* experiment. Each image of Fig. 7 has a displayed dynamic range of 30 dB. The maximum fundamental Doppler signal, Fig. 7b, is 12 dB higher than the maximum power Doppler signal, Fig. 7a but, also, exhibits pronounced blooming around the portal vein and other vessels. The maximum second harmonic Doppler signal, Fig. 7c, is 20 dB below the maximum fundamental signal, but exhibits less blooming artefact. Table 1 lists the mean power of the Doppler signal for the regions illustrated in Fig. 7. The clutter signals of the ROIs in Fig. 7 are the mean power of the prewall-filtered signals. The harmonic signal has the lowest clutter levels, but also has the lowest signal levels while experiencing the highest attenuation in depth, due to intervening tissue and microbubbles. The fundamental flow signal has the highest SNR of the three methods, with 30-dB less clutter relative to conventional power Doppler.

Figure 8 shows the results of combining the three processing paths of Fig. 2 into one image. The copper background of Fig. 8 displays conventional pulse in-

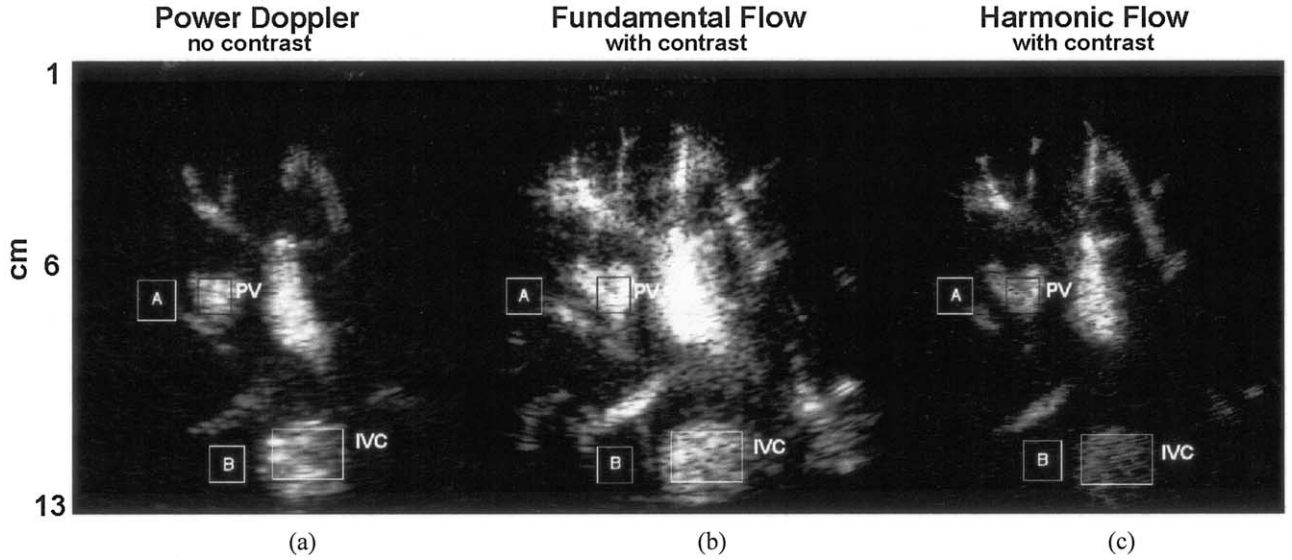

Fig. 7. Power Doppler images of a liver with a dynamic range of 30 dB. The four marked regions are (A) and (B) clutter, (IVC) inferior vena cava and (PV) portal vein. (a) Conventional color Doppler without contrast at MI 1.2, (b) fundamental vascular flow with contrast at MI 0.07, and (c) harmonic vascular flow with contrast at MI 0.07.

Table 1. Mean power of the Doppler signal in the four regions marked in Fig. 7

Flow/signals	Portal vein (dB)	Clutter(A) (dB)	IVC (dB)	Clutter(B) (dB)
Power Doppler without UCA (Fig. 7a)	21	72	17	50
Fundamental flow with UCA (Fig. 7b)	29	40	24	30
Harmonic flow with UCA (Fig. 7c)	18	22	9	12

version processing (Fig. 6). The foreground in blue illustrates a combination of the fundamental and harmonic flow signals shown in Fig. 7b and c. This combination varies with depth, where the second harmonic signal is weighted more at shallow depths and the fundamental flow signal is weighted increasingly at deeper depths. The complementary benefits of both the harmonic and fundamental flow signals are utilized together.

CONCLUSION

Using a pulse-inversion acquisition, a method was described that discriminates between higher-velocity microbubbles in the vasculature and lower-velocity microbubbles in the microcirculation. The method uses the same acquisition for both flow and perfusion. The signal-to-clutter ratios for both the fundamental (−11 dB) and harmonic (−4 dB) vascular flow signals were greater than with conventional power Doppler (−51 dB) without contrast agents (Table 1). The fundamental Doppler image from microbubbles exhibited the greatest SNR and penetration, but suffered from blooming around larger vessels. The harmonic Doppler image exhibited less blooming than the fundamental image, but experienced less penetration and SNR. The complementary traits of the fundamental and harmonic signals were combined to image vascular flow. A low-MI pulse-inversion sequence is processed separately to image simultaneously both perfusion and higher-velocity vascular flow. This method adds information to a conventional contrast examination for perfusion and simplifies the visualization of vascular flow in a contrast examination.

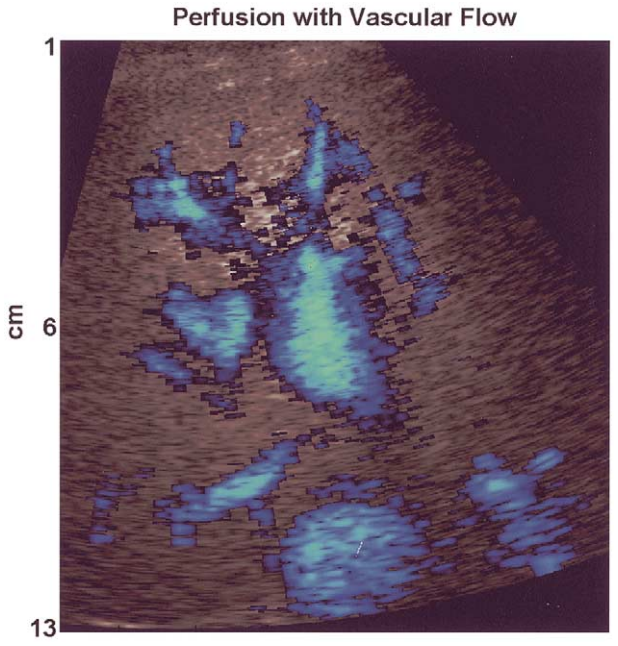

Fig. 8. Perfusion background with vascular flow foreground image with contrast. Vascular flow component is a depth-varying combination of fundamental and harmonic signals seen in Fig. 7a and b.

Acknowledgments—The first author would like to thank Marla Paun, Seth Jensen, Orpheus Kolokythas, Carlos Cuevas and Martin Anderson. The support of Philips Medical Systems is acknowledged.

Averkiou MA. Tissue harmonic imaging. Proc IEEE Ultrason Sympos 2000;2:1563–1572.

Averkiou MA, Powers JE, Bruce MB, Skyba DM. Realtime ultrasonic imaging of perfusion using ultrasonic contrast agents. US Patent 6,171,246 2001.

Bjaerum S, Torp H, Kirstoffersen K. Clutter filter design for ultrasound color flow imaging. IEEE Trans Ultrason Ferroelec Freq Control 2002;49:204–216.

Bruce M, Averkiou M, Powers J. A generalization of pulse inversion Doppler. Proc IEEE Ultrason Sympos 2000;2:1903–1906.

Chomas JE, Dayton PA, May DJ, Ferrara KW. Threshold of fragmentation for ultrasonic contrast agents. J Biomed Opt 2001;6: 141–150.

Evans DH, McDicken WN. Doppler ultrasound: Physics, instrumentation and signal processing. New York: John Wiley & Sons, 2000.

Hope Simpson D, Chin CT, Burns PN. Pulse inversion Doppler: A new method for detecting nonlinear echoes from microbubble contrast agents. IEEE Trans Ultrason Ferroelec Freq Control 1999;46:372–382.

Pohl C, Tiemann K, Schlosser T, Becher H. Stimulated acoustic emission detected by transcranial color Doppler. Stroke 2000;31:1661–1666.

Powers JE, Burns PN, Souquet J. Imaging instrumentation for ultrasound contrast agents. In: Nanda N, Schlief R, Goldberg B, eds. Advances in echo imaging using contrast enhancement. Dordrecht, Holland: Kluwer Academic Publishers, 1996.

Tiemann K, Veltmann C, Ghanem A, et al. The impact of emission power on the destruction of echo contrast agents and on the origin of tissue harmonic signals using power pulse-inversion imaging. Ultrasound Med Biol 2001;27:1523–1533.

Wilson LS. Description of broad-band pulsed Doppler ultrasound processing using the two-dimensional Fourier transform. Ultrason Imaging 1991;13:301–315.

Wilson S, Burns SN. Liver mass evaluation with ultrasound: The impact of microbubble contrast. Semin Liver Dis 2001;21: 147–159.